Macromolecular Research, Vol. 13, No. 3, pp 194-205 (2005)

New Functional Conductive Polymer Composites Containing Nickel Coated Carbon Black Reinforced Phenolic Resin

Farid El-Tantawy

Department of Physics, Faculty of Science, Suez Canal University, Ismailia, Egypt

Nadia Abdel Aal

Department of Chemistry, Faculty of Science, Suez Canal University, Ismailia, Egypt

Yong Kiel Sung*

**Department of Chemistry, College of Science, Dongguk University, Seoul 100-715, Korea*

Received December 16, 2004; Revised April 30, 2005

Abstract: The network structure of Ni-coated carbon black (NCB) composites filled with phenolic resin was investigated by means of using scanning electron microscopy, viscosity, interfacial tension, shrinkability, Flory-Huggins interaction parameters, and swelling index. The electrical properties of the composites have been characterized by measurement of the specific conductivity as a function of temperature. Additionally, the variation of conductivity with temperature for the composites has been reported and analyzed in terms of the dilution volume fraction, relative volume expansion, and barrier heights energy. The thermal stability of phenolic-NCB composites has been also studied by means of the voltage cycle processes. The experimental data of EMI wave shielding were analyzed and compared with theoretical calculations. The mechanical properties such as tensile strength, tensile modulus, hardness and elongation at break (EB) of NCB-phenolic resin composites were also investigated.

Keywords: Ni-coated carbon black composites, polymer matrix, microstructure, electrical property, stability, mechanical property, electro-magnetic wave shielding effectiveness.

Introduction

Conducting polymer composites have been the subject of much interest not only from fundamental scientific view point, for various functional applications.[1-4] The increasing request for thermistors, current switching, temperature controllers, electrofusion welding, electromagnetic interference shielding and lightning protection (static charge) are pushing many researchers to explore new concepts and related materials.[5-9] Thermistors are thermally sensitive resistors. Most thermistors exhibits a decrease in conductivity with an increase in temperature and are referred to as negative temperature coefficient of conductivity (NTCσ) type. Thermistors are widely used in industries for self-regulating heaters, temperature controls, compensation in electronic devices, degassers, etc. especially as overflow protection devices and precise temperature controllers.[10-15] Typical problems associated with thermistors are stability and reproducibility, which become even more pronounced at relatively high temperature and long reliability under severe operation process. Therefore commercialization of high temperature thermistors is yet too realized. However, all electrical and electronic devices emit electromagnetic signals. During recent years, the concerns have grown increasingly about the electromagnetic interference shielding effectiveness (EMI), and the effect on human body of electromagnetic wave radiation from electronics devices. Human tissues may be accidentally or intentionally exposed to electromagnetic sources, cellular mobiles, radars, microwave oven, industrial microwave equipments and others.[16-20] Generally, EMI shielding by absorption rather than reflection is more important for many applications at the present time. Metals or materials coated with metals possess very high EMI ranging from 40 to 100 dB. However, they cannot be used as an electromagnetic wave absorbent since their shallow skin depth makes them shield EMI mainly through the surface reflection.[21,22] On the other hand, electrically conducting polymers are capable of not only reflecting but absorbing the electromagnetic wave and therefore exhibit a significant

*e-mail: yksung@dongguk.edu

1598-5032/06/194-12

advantage over the metallic shielding materials.[23,24] With the above consideration in our mind, we report a novel approach to enhancing the physico-chemical properties of conducting filler into phenolic resin matrix. Our approach is based on the coated of carbon black with nickel metal, which is a precursor on conducting filler of phenolic matrix. In this study the influence of NCB content on physico-chemical properties of phenolic resin composites is addressed.

Experimental

The insulating matrix polymer consists of phenolic resin (resole-type), purchased from (Kuk Do Chemical Industry Co., LTD, Korea). Carbon black (CB) with particle size 8 μm and surface area 90 m^2g^{-1} was obtained from (Fluka A.G) and used as received. Nickel coated CB powders (CB-10 vol% Ni) were prepared using a CB powder and analytically pure $Ni(NO_3)_2 \cdot 6H_2O$ and NH_4HCO_3. $Ni(NO_3)_2 \cdot 6H_2O$ and CB were first mixed in ethanol by alumina ball milling for 2 days. Next, NH_4HCO_3 solution of 1.0 mol was added drop wise to the above slurry under vigorous magnetic stirring for 12 h with controlled the pH at 11 by using excess NH_4HCO_3. The resulting precipitates were filletered by using distilled water and then dried at 100 °C for 1 day on electrical oven. The as dried powders were calcined at 500 °C for 10 h and then the as-calcined samples were reduced at 750 °C for 5 h in hydrogen atmosphere. Several batches of nickel coated carbon black (NCB)/phenolic weight ratios are: 90/10, 80/20, 70/30, 60/40 and 50/50 respectively and abbreviated as NCB10, NCB20, NCB30, NCB40, and NCB50 respectively. The green phenolic with different content of NCB was prepared by centrifuging mixer for 2 min at room temperature. The bulk samples of composite were obtained by casting the green composites on Teflon mould. Before the specimens were cured, the phenolic resin was debunked by removing all entrapped air bubbles using a hot plate. The temperature of the hot plate was kept at 55 °C to achieve minimum viscosity of the resin. Once the air bubbles were removed, the specimens were transferred to a hot press for curing for 2 h under uniaxial pressure 200 KN/m^2 and temperature 150 °C. The shrinkability (S) can be calculated from the weight determinations as follows[2,18]:

$$S(\%) = \frac{\rho_{th}}{\rho_c} \times 100 \tag{1}$$

where ρ_{th} is the theoretical density of the component and ρ_c is the density of the composites. The ρ_c was measured by Archimedes principle. The composite samples were first weighted dry (w_0) and dipped into water for 2 h, then weighted again after fluid immersion(w_1), and finally weighted while immersed in water (w_2). Then the ρ_c is given by:

$$\rho_c = \frac{w_0}{w_1 - w_2} \times \rho_{water} \tag{2}$$

Morphology study of the phenolic composites was conducted on scanning electron microscopy SEM, (s-4100, Hitachi, Tokyo, Japan). The interfacial tension (γ) of composites was tested by contact angle measurements using a (CA-2000, Tokyo, Japan) contact angle meter. The viscosity of the composites was measured by using viscometer analyzer (VS-100, Tokyo, Japan). The thermal volume expansion coefficient $V(T)$ was measured by a dilatometer technique as described elsewhere.[5] The dilution of volume fraction $D_{VF}(T)$ is related to the relative thermal volume expansion $V(T)/V_0$ by the following equation[19]:

$$D_{VF}(T) = \frac{f \cdot e}{(1-f)e^{V(T)/V_0} + f \cdot e} \tag{3}$$

where V_0 is the initial volume of the NCB composite at room temperature and f is the filler volume fraction at room temperature.

For electrical characterization, Cu-electrodes were embedded into samples during preparation process to reduce the sample- electrode contact resistance.[1,17] The bulk electrical conductivity (σ) was measured using a Multi-Mega–Ohmmeter type MOM12 and a measuring cell ODW2 (from WTW Co., Germany). The data were automatically collected using a suitable interface and data acquisition pc code. Conductivity was calculated from current-voltage characteristics using the following equation: $\sigma = (IL/VA)(\Omega cm)^{-1}$, where I is the current, L thickness of the sample, A area of the sample and V is the voltage applied. For the measurement of the potential–dependent temperature, the sample was placed in controlled chamber at 20 °C. Computer controlled the temperature for each applied potential.

Thermoelectric power (TEP) seebeck coefficient was measured in air by steady - state temperature gradient method.[1] The TEP was evaluated by correcting the linear gradient of TEP=$\Delta F/\Delta T$ for thermo-power of platinum, where ΔF and ΔT are the thermo-electromotive force and temperature difference between both ends of sample measured with Pt leads and Pt/Pt-Rh thermocouples, respectively. The dielectric properties were calculated from the capacitance measurements made using a Hewlett Packard 4994-A impedance analyzer at room temperature in the frequency range from 1 KHz to 10 GHz. The static energy (SE) of the composites was measured with a static charge meter (AX-221, Tokyo, Japan). For measuring the discharge properties the tested samples were charged in a 15 kV electric filed (corona discharge). The discharge voltage time dependence was displayed by using an integration electrometer. The electromagnetic wave shielding effectiveness properties were also determined by the Hewlett-Packard waveguide line in which has containing spectro-analyzer, power meter,

reflection meter, and attenuation meter. The measurements were carried out in the frequency ranges 1.0-15 GHz. The thickness of the testing sample was about 1 mm. The mechanical properties of the samples were determined using a testing instrument Instron, UK. Hardness (H_v) has been determined using a universal testing machine (ASTM-D2240-78).

Results and Discussion

Morphological and Network Structure of the Composites. The scanning electron microphotograph (SEM) of the phenolic resin-NCB composites of samples NCB10 and NCB50 are shown in Figure 1(a) and 1(b), respectively. The micrograph of sample NCB10 consists of gallery space in the resin into composites matrix and the density of resin is higher. On the other hand, the micrograph of sample NCB50 exhibits a good interface adhesion between NCB and resin matrix, and the NCB particles are more tight contacts through the composites forming effective conducting network structure. The SEM results are also analyzed from the point of view of packing density. The NCB50 sample, show a progressive improvement with respect to particle-to-particle connectivity (i.e. high packing density and aspect ratio). The average particle size observed from the scanning micrographs is about 9 micron. In order to confirm this observation, the interfacial tension (γ), viscosity(η), and shrinkability(S) as a function of NCB content has been analyzed and is plotted in Figure 2(a). It is clearly that both the γ, η, and S increases with increasing NCB content in the composites. The increment of γ is due to the fact that the NCB particles are well wetted by phenolic resin and have been bonded to molecules of the resin with intensive physical and chemical bonds.[5] While the increment in η values with increasing NCB loadings indicates that as more and more NCB particles gets into the resin matrix and the mobility of the macromolecular chains of the resin reduces resulting in more rigid composites.[3] The S increases with increase NCB content in the composites. It is tempting to speculate that when the NCB increases the entanglement network structure increases (i.e. the void formation decreases) with NCB addition into the composites as confirmed by SEM photographs above. To gain more deep light on the influence of NCB content on the network structure, the number of elastically effective chains (NEC) of the composites has been estimated using the relation[20]:

$$NEC = \frac{\rho_r N_A}{M_a} \tag{4}$$

where ρ_r is the polymer density, N_A is the Avogadro's number and M_a is the average molecular weight of polymer between crosslink's, and is calculated by the following relation[1,21]:

(a)

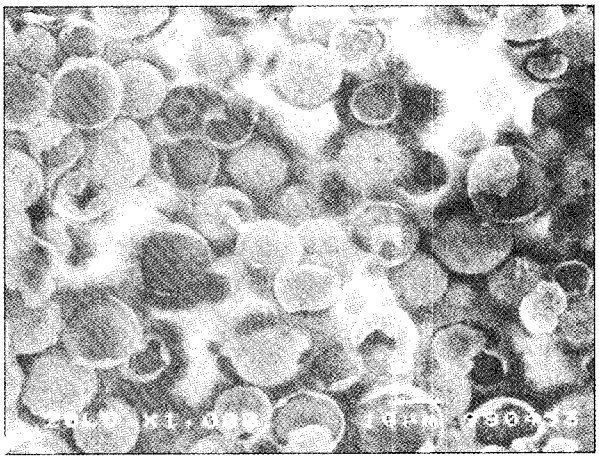

(b)

Figure 1. The scanning electron microphotograph (SEM) of the phenolic resin - NCB composites: (a) samples NCB10 and (b) NCB50.

$$M_a = -\frac{\rho_r V_s V_{rf}^{1/3}}{\ln(1-V_{rf}) + V_{rf} + \chi V_{rf}^2} \tag{5}$$

where V_s is the molar volume of solvent, χ is the Flory-Huggins interaction parameter between solvent and polymer and is given by[6]:

$$\chi = \theta + \frac{V_s(\delta_s - \delta_p)^2}{RT} \tag{6}$$

where θ the lattice constant, δ_s and δ_p the solubility parameter of solvent and polymer respectively, R the universal gas constant, T the absolute temperature and V_{rf} the volume fraction of polymer in the solvent swollen filled sample and is given by[15]:

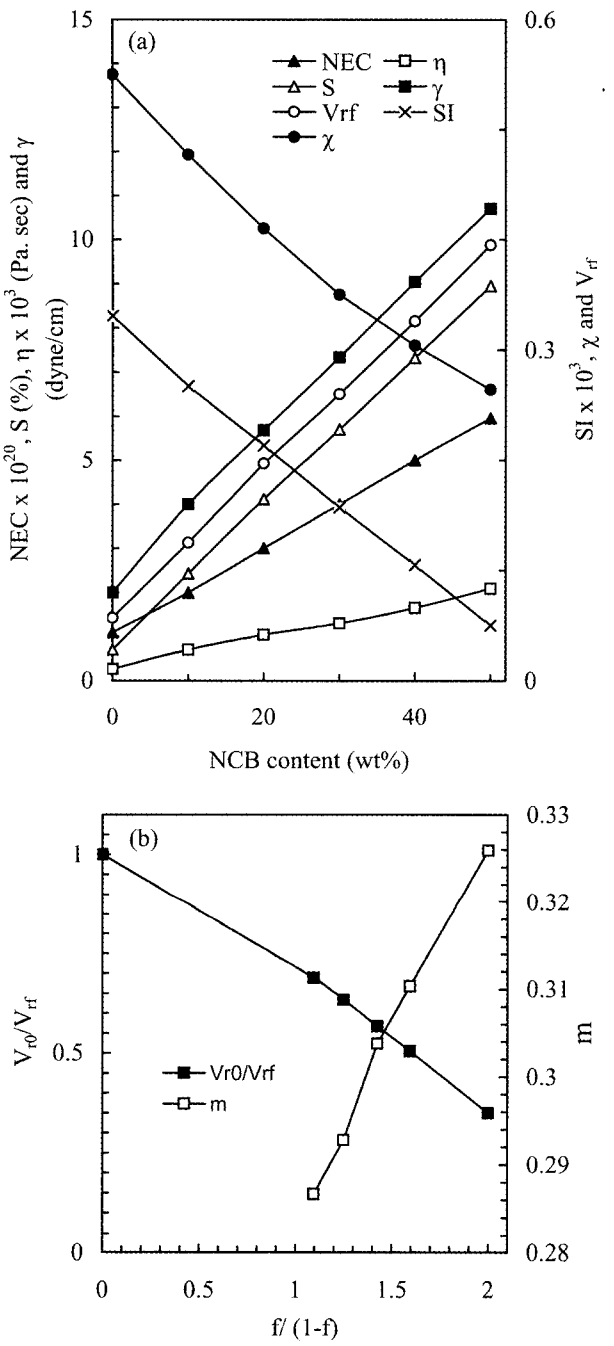

Figure 2. (a) γ, η, S, NEC, V_{rf}, χ, and SI of phenolic resin composites versus the NCB content and (b) variation of V_{r0}/V_{rf} and with $(f/1\text{-}f)$ of phenolic resin composites.

$$V_{rf} = \frac{(d - fw_0)\rho_p^{-1}}{(d - fw_0)\rho_p^{-1} + A_s\rho_s^{-1}} \tag{7}$$

where d the deswollen weight of sample, w_0 the initial weight of sample, A_s the amount of solvent absorbed by sample and ρ_p is the density of solvent.

The swelling index (SI), which is a measure of the swelling resistance of polymer composite, is calculated using the equation[22]:

$$SI(\%) = \frac{A_s}{w_0 \times 100} \tag{8}$$

Figure 2(a) shows the NEC, V_{rf}, χ, and SI of phenolic resin-NCB composites versus the NCB content. The augmentation of NEC, can be ascribed to the NCB favors the formation of an effective chains network across the matrix and forms more links branches within the composite network. Also, it is found that the V_{rf} increases with increasing NCB content. This indicates that NCB is a better adhesion and higher extent of interaction between NCB particles and resin matrix. The relationship between SI and χ as a function of NCB content is also presented in Figure 2(a). It is seen that the SI decreases with increasing NCB content. This indicates that the intermolecular distance decreases with NCB loading level and the solvent uptake also decreases. Furthermore, as loading increase the amount of solvent absorbed by sample decreases which lead to decrease in χ values and in turn increases the interaction between filler and matrix. The polymer–filler interaction parameter (m) is given by[23]:

$$\frac{V_{r0}}{V_{rf}} = 1 - m\left(\frac{f}{1-f}\right) \tag{9}$$

where V_{r0} the volume fraction of green phenolic vulcanizates. The value of m is calculated from the slope V_{r0}/V_{rf} versus $(f/1\text{-}f)$, as example in Figure 2(b). It is seen that the V_{r0}/V_{rf} decreases with increasing NCB content in the composites. This behavior leads to a negative slope indicating the reinforcement effect of NCB particles within resin composites.[13] It is interesting to note that the m values increase with increasing NCB content into the composites as shown in Figure 2(b). This fact supports that the inclusion of NCB particles improves the molecular structure and increase the excluded volume (i.e., the molecular connectivity) of the composites.

Insulator – Conductor Transition. The resistivity (ρ), μ and TEP of phenolic-NCB composites were determined in Figure 3 as a function of the NCB weight fraction. Phenolic resin is electrically nonconductive and has a bulk conductivity about 10^{-15} (Ohm cm)$^{-1}$ in dry state at room temperature. The resistivity of composites increases with NCB content into phenolic matrix and shows an S-shaped profile. When the NCB particles are lowering dispersed into resin matrix, fewer particles-particles can be formed, resulting in a lower conductivity of the composites. The conductivity increases much with increasing volume fraction of NCB particles. This may be the dispersion of NCB grains and increase of adhesion force between NCB and resin matrix. The more

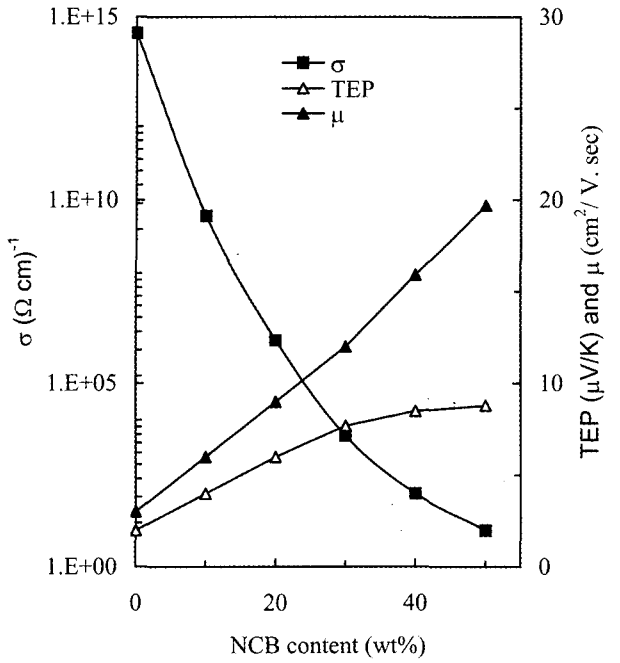

Figure 3. The resistivity, μ and TEP of phenolic-NCB composites as a function of the NCB content.

extreme the links of the NCB particles-resin is, the larger its excluded volume was. The larger the excluded volume is, the higher the resistivity of the composites. In Figure 3 it is seen that the μ increases with increasing NCB. This demonstrates that the NCB particles promote charge carriers transport between polymer chains by this means improve the composites conductivity. Also, the charge carriers promote to induce the interfacial force among NCB and resin matrix. The percolation threshold in the composites is about 13 wt% of which is much smaller than that of conventional conducting macro composites.[1-3] This result is consistent with non-universal conducting polymer composites.[12] However, the relation between composite conductivity (σ_m) and conductivity of NCB content (σ_f) in the viciency of the critical percolation threshold can be described by the following equation[24]:

$$\sigma_m = \sigma_f(f-f_c)^N \tag{10}$$

where f_c is the onset conduction or percolation threshold and N is a constant determining the power law-conductivity behavior.

The calculated value of N for NCB-phenolic resin composites is about 4.03. The high value of N indicates that the non-universal transport behavior and conduction in the composites have controlled by tunneling process.[1-4] In Figure 3, it is clear that the TEP is a negative values and increases with increasing NCB content in the composites up to the percolation threshold and then slightly increased. The negative values of TEP for NCB composites mean that the conduction is controlled by electron. It is worthily that the TEP above the f_c was not depend on content of NCB particles. This indicates that the conducting network by NCB is formed at the loading level higher than the f_c.

Negative Temperature Coefficient of Conductivity (NTCσ) Thermistors. A more important feature of this kind of conducting polymer composite is the negative temperature coefficient of the conductivity (NTCσ). Figure 4(a) shows the variation of electrical conductivity (σ) of the NCB-phenolic composite samples with temperature in the range of room temperature to 150 °C. It is seen that as temperature increases, the conductivity decreases first slowly, and then at a switch temperature, falls abruptly decreases. This is attributed to a lowered real NCB volume fraction (i.e. a diluted NCB composition) due to the increase of thermal volume expansion of the resin matrix as confirmed by measured the relative thermal volume expansion $V(T)/V_0$ and dilution volume fraction $D_{VF}(T)$ versus temperature as shown in Figure 4(b). Additionally, we believe that with increasing temperature the height of the energy barriers (ϕ_E) increases along the grain boundary of the composites and thereby the conductivity decreases. The energy barrier is given by the equation[6]:

$$\phi_E = \frac{e^2 N_s^2}{8\varepsilon_0 \varepsilon_r N_d} \tag{11}$$

where N_s is the interface state density, N_d is the carrier density in the composites, ε_0 is the dielectric constant of composite in vacuum, ε_r is the effective dielectric constant of the composites in air and e is the electronic charge.

Figure 4(c) shows the variation of ϕ_B versus T of NCB-resin composites. It seen that the ϕ_B of composites increased with the increased T. A possible explanation is that with increase of temperature the contact between conductive particles, i.e., grain boundary area, increased. Thereat the relative frequency of electrons scattering increases, and their energy barrier increases, resulting in a decrease of conductivity.

However, from σ-T curve, a temperature coefficient (ψ) of NTCσ thermistor is defined as:

$$\psi = \frac{\partial \log \sigma}{\partial T} \tag{12}$$

Also, the value of thermistor constant (B) for a practical thermistor material can be found by measuring the resistivity at two values of absolute temperature T_1 and T_2 by using the following equation[14]:

$$B = 2.303\left(\frac{T_1 T_2}{T_2 - T_1}\right)(\log T_{T1} - \log \rho_{T2}) \tag{13}$$

where ρ is the resistivity of NTC composites.

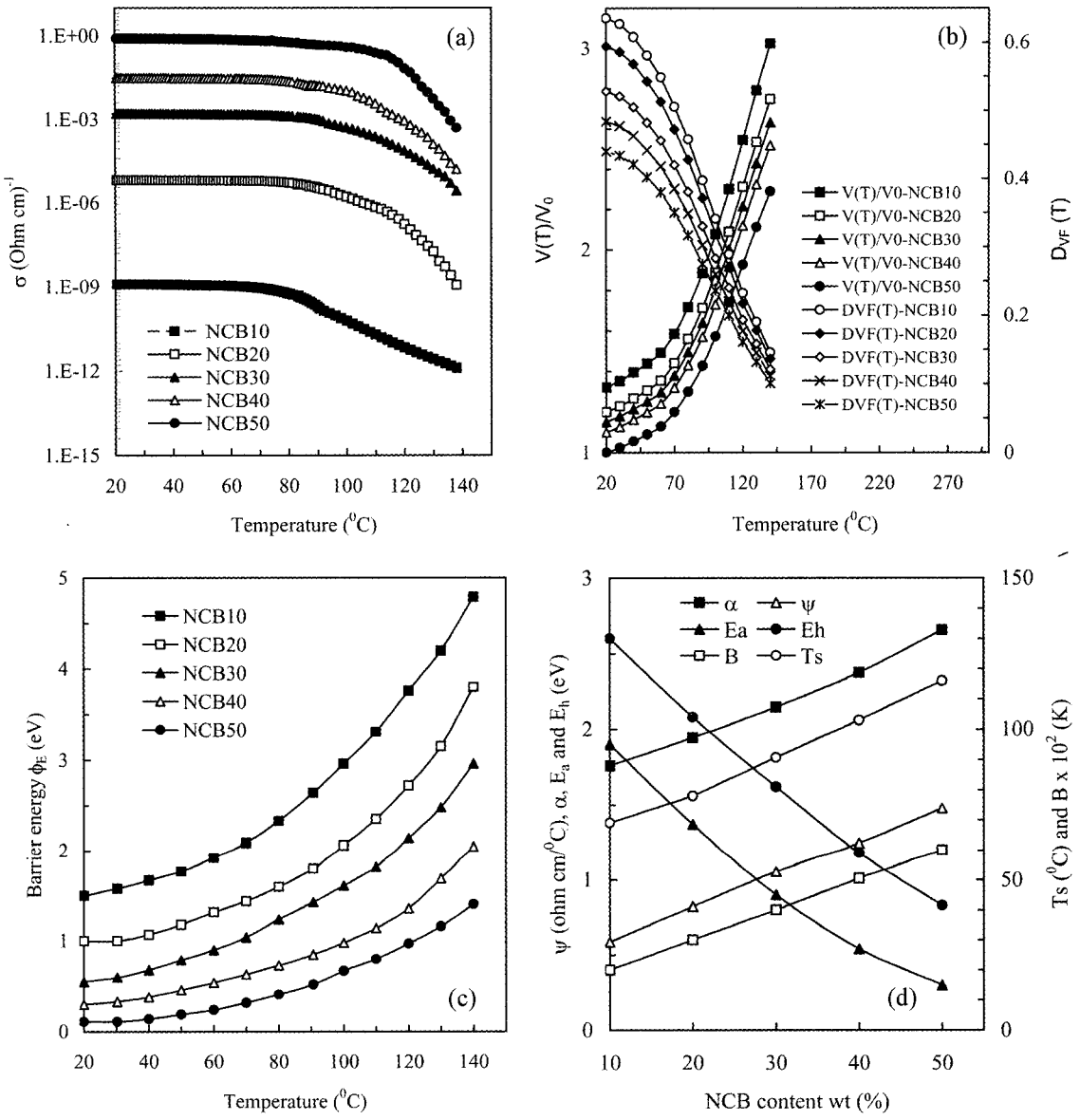

Figure 4. (a) Variation of σ of the NCB-phenolic composite samples with T in the range of room temperature to 150 °C, (b) variation of relative thermal volume expansion $V(T)/V_0$ and dilution volume fraction $D_{VF}(T)$ versus T of phenolic composites, (c) variation of ϕ_E versus T of NCB-resin composites, and (d) variation of ψ, B, T_s, α, E_a, and E_h on volume fraction of NTC content.

The predicted switch temperature (T_s) can be also determined at a temperature as the following:

$$\left(\frac{\partial^2 \log \sigma}{\partial^2 T}\right)_{T=Ts} = 0 \tag{14}$$

The dependence of ψ, B, and T_s on volume fraction of NTC content in the composites is plotted in Figure 4(d). It is clear that the T_s is shifts to a higher temperature with increasing NCB content. Larger B and ψ values correspond to higher thermal-electrical switch rates. Above Results show that 20 to 50 v/v fraction of NCB loading makes the resin composite a potential NTC σ thermistor material for use in the electronics industry with high quality microstructure and good thermal stability.

Applicability of Conduction Mechanism to the Composite Systems. According to the variable range hopping theory, conductivity depends on temperature in the form:

$$\sigma(T) = \sigma_0 \exp\left[-\left(\frac{T_c}{T}\right)^Y\right] \tag{15}$$

where σ_0 and T_c are constant and Y is a parameter which is

related to the dimensionality by $Y = 1/(d_s + 1)$.

The conductivity data fits the straight line only when $\ln\sigma$ values were plotted against $T^{-1/4}$. This result supports that the mechanism of conductivity is 3-dimentional tunneling of electrons inside resin matrix.[1-3] To confirm the above fact we attempt to computed the activation energy (E_a) and hoping energy (E_h) by using the following equations:

$$\sigma = \sigma_1 \exp\left(-\frac{E_a}{KT}\right) \tag{16}$$

and

$$\sigma T^{\frac{1}{2}} = \sigma_0 \exp\left(\frac{E_h}{KT}\right) \tag{17}$$

where σ_1 and σ_0 is the pre-exponential factor and K is the Boltzmann constant.

The estimated values of E_a and E_h vs. NCB content are recorded in Figure 4(d). It is seen that the values of E_a and E_h are not the same for the composites. This indicates that the conductivity is controlled by conduction mechanism of the tunneling process as confirmed before.

Applicability of the Composites as Current Switching and Plastic Welding. The current-voltage (I-V) characteristic of NCB-phenolic composites is presented in Figure 5. From the I-V characteristic it can be seen that at low applied voltage there is no nonlinearity at all. At relatively higher voltage there are nonlinear behaviors. This is attributed to with increasing applied voltage, the electrical power dissipation in the composite leads to rise in body temperature. Thereby, a self-heating in the composite is due to the localized thermal effects. It is to note that the I-V characteristics for the NCB composites show the turn – on current (i.e. current switching) at certain voltage depending on NCB content. The observed difference in current switching values is due to the variation of the microstructure and the degree of crosslinking density of the composites.

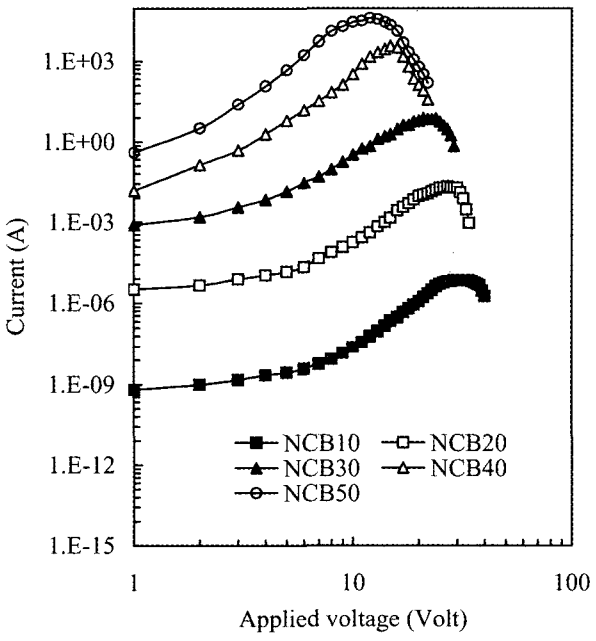

Figure 5. Current-voltage (I-V) characteristic of NCB-phenolic composites.

The nonlinear behavior curve can be determined by using the following formula[15]:

$$\alpha = \frac{\log(I_2/I_1)}{\log(V_2/V_1)} \tag{18}$$

where I_1 is the current at the voltage V_1 and I_2 is the current at the voltage V_2.

The estimated values of α as a function of NCB content are plotted in Figure 4(d). The increase of α indicates that these NCB improve the crosslinking density and molecular texturing of the phenolic matrix.

For welding applications, it is well know that the welding principle using conductive polymer composites, is usually as films, is comparable with resistance welding like electrofusion welding of thermoplastics.[9] The conductive composites used for the films are mostly the same as the plastics to be welded. The welding procedure is the same as electrofusion welding.[10] The welding properties of the NCB composites are listed in Table I. A close look to the data in Table I, it is seen that the samples NCB10 and NCB20 have a higher resistivity, welding voltage and time. While the samples NCB30, NCB40, and NCB50 have low resistivity, welding voltage and time. Therefore, we recommended using the samples NCB40 and NCB50 as a welding material because the welding voltage is absolutely safe and the welding time is acceptable practically with good thermal stability.

Applicability of the Composites as Temperature-Voltage Controls. The study of the temperature–voltage characteristics of the NCB composites thermistors and determination of the optimum temperature are very important from the point of view of producing reliable thermistor, in which a priori knowledge of ultimate temperature to fix the upper limit of applied potential within which the thermistors can be operated safely without any performance degradation. The

Table I. The Welding Properties of NCB-phenolic Resin Composites

Sample Code	Welding Voltage (volt)	Welding Time (sec)
NCB10	200	240
NCB20	120	180
NCB30	70	50
NCB40	40	21
NCB50	25	13

dependence of temperature of composites on applied voltage is shown in Figure 6. It is clear that the temperature increase with increasing applied potential and strongly depends on NCB content. The incorporation of NCB into the resin matrix had increased the maximum temperature level of phenolic resin composites. In other words, the lower the composite resistance, the higher the heat-up rate and the lower the voltage applied. We believe that with increasing applied voltage, the electrical field dissipation in the com-posite leads to a rise in body temperature. Thus a self–heating phenomenon in the composites is due to the localized thermal effects. A linear dependence of temperature on the applied voltage is observed for NCB contents up to 20 wt% in the composites. The linear behavior of the temperature as a function of the applied voltage demonstrates their potential application for temperature controls.

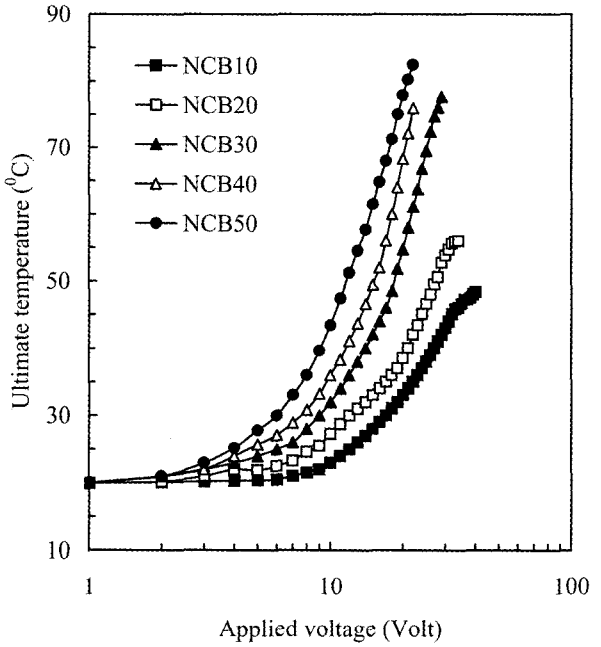

Figure 6. Dependence of temperature of composites on applied voltage.

Thermal Stability of the Composites. The durability of the thermistors is evaluated by subjecting the thermistors to the applied voltage cycles test. Figure 7(a) displays the temperature-time curve in presence of an external applied voltage of about 20 volt on and off for NCB10 and NCB50 sample. One can observe that there is no significant change in the maximum temperature upon several cycles for NCB50 sample. While at low volume fraction of NCB, i.e., NCB10, there is an increase of temperature with increasing cycle order. The bulk temperature of the composites is increased rapidly until dipping time 3 min, depending on NCB content, after 3 min it reaches an equilibrium temperature. But the bulk temperature at equilibrium of the composites is increased with increasing NCB content. The results could be explained by NCB particles forming more compact cross-linking structures in the composites. Thus, the composite at high loading had a thermal stability. However, the tempera-ture-time curve in Figure 7(a) can be described by the exponential growth relation[5,6]:

$$(T-T_0) = (T_m-T_o)(1-\exp-(t/\tau_g)) \quad (19)$$

where T_m and T_0 are the maximum and initial temperature respectively and τ_g is the characteristics growth time constant depends on NCB content and is calculated at $t_g = \tau$.

The estimated values of τ_g as a function of NCB content

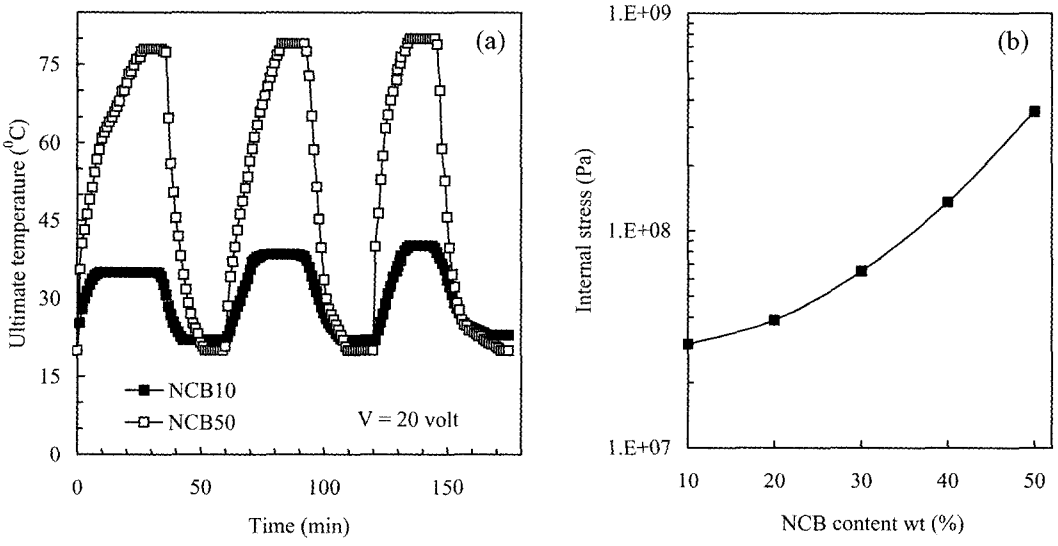

Figure 7. (a) Temperature-time curve in presence of an external applied voltage of about 20 volt on and off for NCB10 and NCB50 sample and (b) Dependence of internal stress in NCB content of phenolic composites.

are 17, 13, 10, 8, 6, and 3 min, respectively. This result indicates that the inclusion of NCB particles into resin matrix increases the cross-linking density and their thermal stability as confirmed by estimated the internal stress of the composites.

It was known that when the thermistor was cooled the volume change and the network structure distortion would occur. Thereby the internal stress (E) would produce in the composites. The value of internal stress is derived from the Young's modulus (Y_{MS}) by the following equation[20]:

$$E = Y_{MS}\exp(-bP) \tag{20}$$

where P is the porosity and b is the material constant is about 6 for our composites.[6]

The variation of internal stress in NCB content of phenolic composites is plotted in Figure 7(b). It is found that the internal stress increase with increasing NCB content. This fact suggests that the NCB acting as a clamping force and thermodynamically stabilizing agent within resin composites as confirmed before.

Applicability of the Composites as Lightening Protection Materials. The energy of the composites as a function of NCB content is plotted in Figure 8(a). It is clear that the energy decreases with increasing NCB content. The values of energy for NCB10 and NCB20 sample are quite acceptable for lighting protection application.[6,10] The discharge voltage of NCB-phenolic resin composites as a function of time is plotted in Figure 8(b). It is seen that, after the time reached 10 s, the voltage of the composites tended to level off with further increasing time. The data in Figure 9(b) can be described by the exponential decay equation as:

$$(V - V_m) = (V_m - V_o)(1 - \exp-(t/\tau_d)) \tag{21}$$

where V_m is the maximum voltage and τ_d is the exponential decay time constant and strongly depend on NCB content and is calculated at $\tau_d = t$.

The computed values of τ_d as a function of NCB content for phenolic composites are presented in Figure 8(a). It is clearly that the values of τ_d for NCB10 and NCB20 sample are quite acceptable for lighting protection (i.e. antistatic charge dissipation). We recommended to use this NCB composite at low loading level i.e. samples NCB10 and NCB20 as lighting protection (antistatic charge dissipation).

Applicability of the Composites as EMI Shielding Effectiveness Materials. It is believed that the network structure and interface adhesion were major factors contributing to improved EMI shielding properties of the filler-matrix composites. The performance of shielding composites can be evaluated by comparing the EMI measurements by theoretical equations as follows[22-24]:

$$EMI(dB) = R + A \tag{22}$$

where R and A are the shielding efficiency due to reflection and absorption respectively.

Each term is explicitly written as:

$$R(dB) = 20\log\left[\frac{0.462}{r\sqrt{\frac{\mu}{f\sigma}}} + 0.316r\sqrt{\frac{f_i\sigma}{\mu}} + 0.354\right] \tag{23}$$

$$A(dB) = 3.34 \times 10^{-3} h\sqrt{f_i \mu_i \sigma} \tag{24}$$

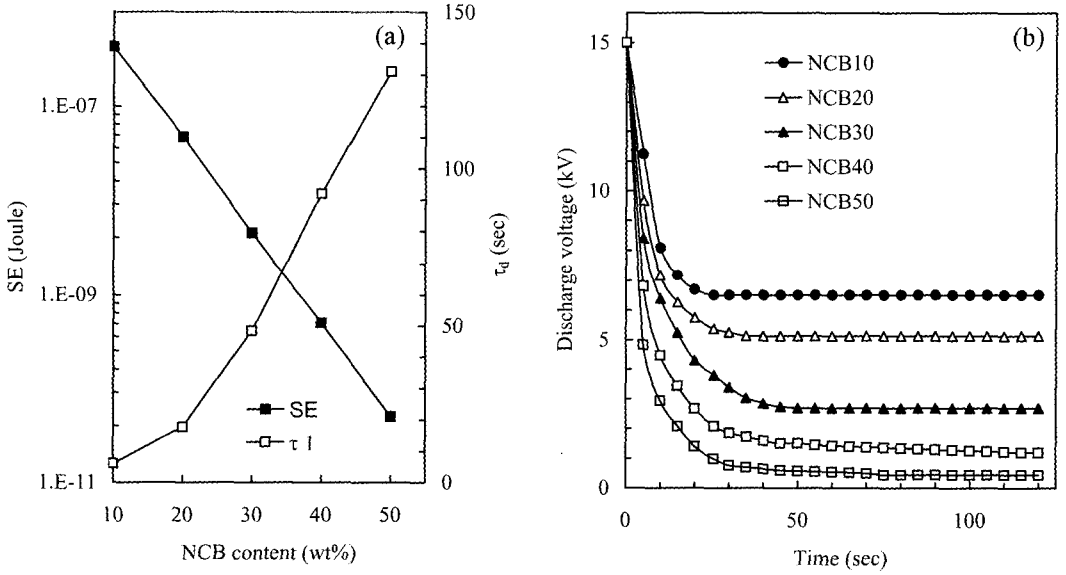

Figure 8. (a) The energy and decay time constant of the composites as a function of *NCB* content and (b) The discharge voltage of the composites as a function of time.

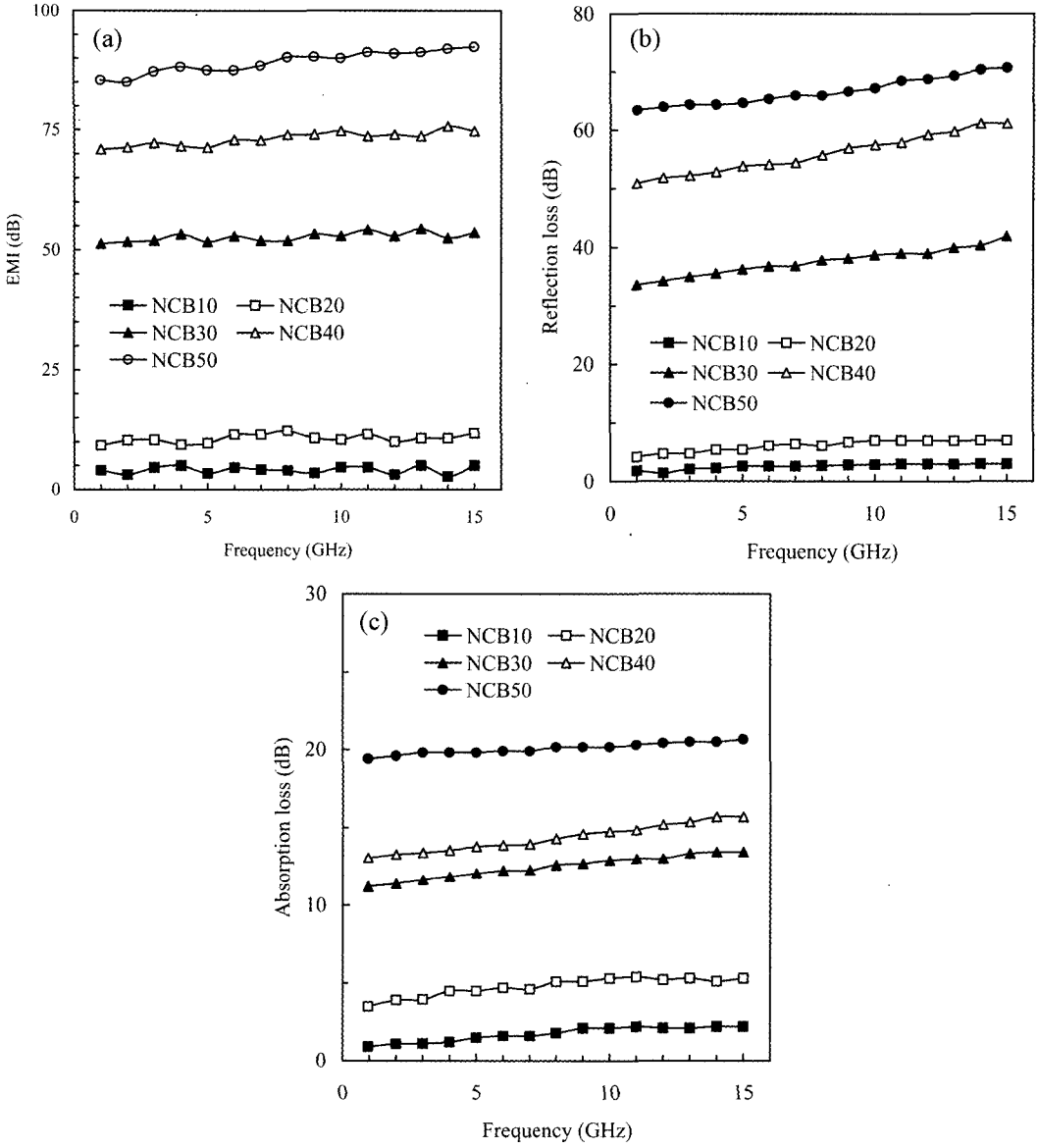

Figure 9. (a) EMI measured against frequency for phenolic composites, (b) computed reflection loss for phenolic composites, and (c) computed absorption loss for phenolic composites.

where r is the distance from the emission source to the shielding material, f_i is the incident frequency, μ_i is the magnetic permeability and h is the thickness of sample.

Figure 9(a) present the EMI measured against frequency for phenolic resin composites. It is seen that the EMI increases monotonically with increasing NCB content, as expected. This indicates that the EMI is governed by the NCB content in the resin composites. With increasing NCB content, the connectivity or interfacial adhesion among conductive phases become more enough (i.e. tight contact) to allow the charge carriers to hop across barriers within resin matrix. The high shielding effectiveness of sample NCB50 is attributed to the high reflectivity of nickel particles and absorption of the composites. The theoretical reflection and absorption shielding effectiveness of the composite are calculated using room temperature DC electrical conductivity is plotted in Figure 9(b) and 9(c), respectively, and the values are compared to the experimental data. The theoretical EMI are approximately in accordance with experimental data. It is found that the EMI shielding increases with increasing σ and dielectric constant of the composites. Figure 10 shows the variation of dielectric constant and dissipation factor as a function of NCB content of resin composites. Both dielectric constant and dissipation factor increase as the NCB content is raised. At low loading level the composites had less constraint force, which resulted in decrease of

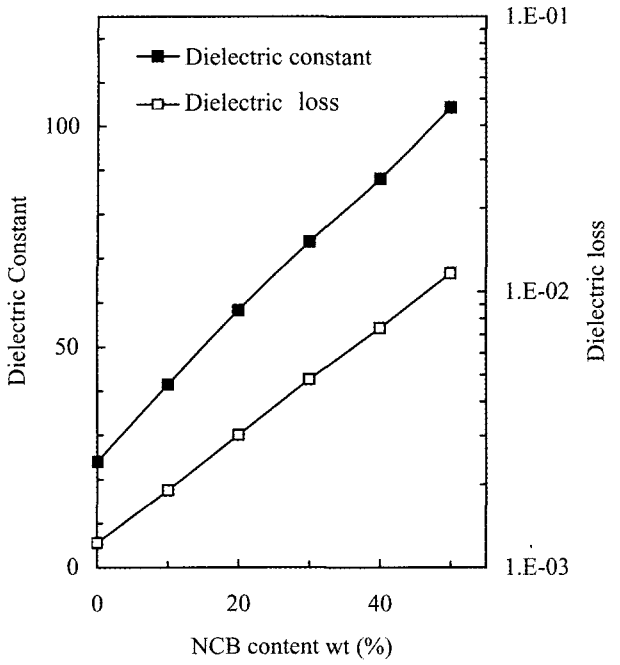

Figure 10. Dielectric constant and dissipation factor as a function of NCB content.

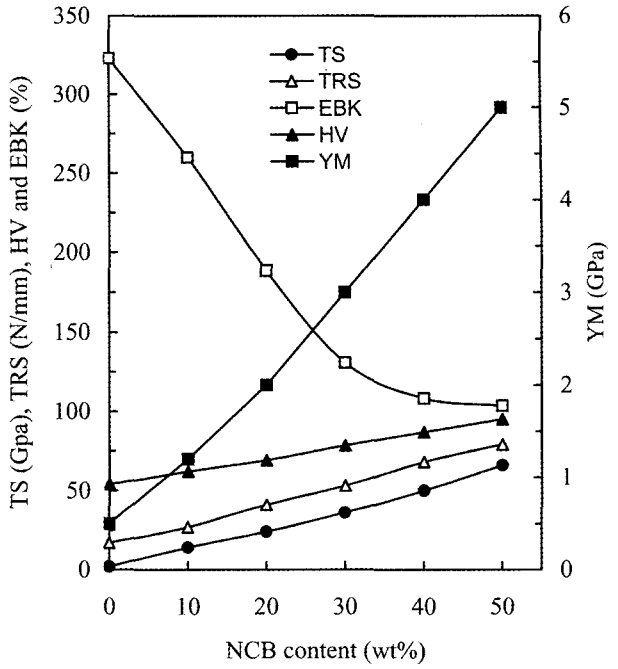

Figure 11. Young's modules (YM), tensile strength (TS), tear strength (TRS), hardness (HV) and elongation at break (EBK) as a function of NCB content.

the internal stress as confirmed in Figure 7(b). At the same time, this was less bonding between individual chains into the composites. As the NCB content is raised, the NCB particles get more tight contact and clusters of particles are formed. The average interfacial polarization associated with a cluster is larger than that of an individual particle, because of the increase in the dimensions of the conducting NCB inclusion. This leads to the increase of the charge carrier density and the EMI shielding of the resin composites.

Mechanical Properties of the Composites. Figure 11 shows the dependence of the Young's modules (YM), tensile strength (TS), tear strength (TRS), hardness (HV) and elongation at break (EBK) on NCB content for resin composites. As expected, the variation of the mechanical properties depends on the amount of NCB in the composites. It is clear that the YM, TS, and TRS, and HV increases with increasing NCB loadings. This increase is primarily due to the entanglement of the NCB particles in the network, which reinforces the composites much more effectively. Another possible reason is probably due to the strong interfacial strength between NCB particles and resin matrix. This strong bonding between NCB and matrix increases the load transfer from the resin matrix to NCB particles. The increase of the tear strength originates from an increase in the crystallinity and rigidity of the resin matrix with increasing filler content as confirmed by viscosity result before. On the other hand, the EBK decreases with increasing NCB content. This is attributed to that with increasing NCB content the resin matrix become stiffer and harder. This leads to decrease the composite resilience and toughness and thereby the EBK decreases. The NCB composites exhibit as both high performance and electrically conductive polymeric material. Therefore, they show functional applications in high temperature conducting adhesive, antistatic coatings, electromagnetic shielding and bipolar plates of polymer electrolyte membranes.

Conclusions

The development of conductive polymer composites comes up a new avenue for the possible application of conductive phenolic resin-NCB composites in a wide range of industries including the negative temperature coefficient of conductivity (NTCσ) thermistors, current switching, temperature sensor, lightening protection, and electromagnetic shielding effectiveness with thermal stability. The present investigation can be summarized as follows:

1. The nickel coated carbon black particles show good distribution, interface adhesion, and acting as a clamping force within resin matrix.

2. The electrical conductivity of the composites decreases with increasing temperature and behaves as negative temperature coefficient of conductivity (NTCσ) thermistors. The conductivity is controlled by the conduction mechanism of tunneling process. The activation and hoping energies are strongly depending on the NCB contents in the composites.

3. The current turn–on with voltage and the linear depen-

dence of the temperature on the voltage is a warranty that these composites can be applied for current switching and temperature controls. In addition, it is worthwhile to note that for welding application, the welding voltage is absolutely safe and the welding time is acceptable practically.

4. The EMI shielding effectiveness is governed by the NCB particles in the resin matrix. The EMI at high loading level reaching 95 dB and this value are higher than all values of the shielding effectiveness that have been previously reported for conventional conducting polymer composites.

5. The mechanical properties increase with increasing NCB loading level and are due to the entanglement of the NCB in the structure, which reinforces the composites much more effectively.

Acknowledgements. This work has been supported by Suez Canal University and Dongguk University.

References

(1) F. El-Tantawy, K. Kamada, and H. Ohnabe, *J. Appl. Polym. Sci.*, **87**, 97 (2003).
(2) F. El-Tantawy, *Eur. Polym. J.*, **38**, 567 (2002).
(3) F. El-Tantawy, K. Kameda, and H. Ohnebe, *Polym. Inter.*, **51**, 635 (2002).
(4) F. El-Tantawy, *Eur. Polym. J.*, **37**, 565 (2001).
(5) F. El-Tantawy, *Proceedings of the 7th Japan International SAMPE Symposium & Exhibition*, Nov. 13-16, 797 (2001).
(6) F. El-Tantawy, and Y. K. Sung, *Proceedings of the 25 Arab School of Science & Technology,* Damascus, Syria, August 28-3 September, 100 (2004).
(7) Y. K. Sung and F. El-Tantawy, *Macromol. Res.*, **10**, 67 (2002).
(8) Z. Jingvhang, L. Longtu, and G. Zhilum, *Sensor. Actuat.*, **A 5**, 3108 (2001).
(9) B. O. Lee, W. J. Woo, and M. S. Kim, *Macromol. Mater. Eng.*, **286**, 114 (2001).
(10) S. Y. Xiao, G. Wu, and Y. Pan, *Polym. Int.*, **44**,117 (1998).
(11) D. C. Hyung, W. S. Hwan, Y. C. Kwng, J. L. Hyuck, S. P. Chan, and G. Y. Ho, *J. Appl. Polym. Sci.*, **72**, 75 (1999).
(12) R. Mihai, S. Nicoleta, and R. Daniela, *Polym. Testing*, **20**, 409 (2001).
(13) J. L. Wan, J. K. Yong, and K. Shinyoung, *Synth. Metal*, **113**, 237 (2001).
(14) Y. H. Chi and C. W. Chang, *Eur. Polym. J.*, **36**, 2729 (2000).
(15) N. C. Das, D. Khastgir, T. K. Chaki, and A. Chakraborty, *Composites, Part A*, **31**, 1069 (2000).
(16) H. S. Sack and M. C. Moriarity, *Solid State Commun.*, **3**, 93 (1995).
(17) S. Y. Xiao, S. Lie, and Y. Pan, *Composites Sci. Tech.*, **61**, 949 (2001).
(18) F. Cespeds, E. M. Fabregas, and A. Alegret, *Anal. Chem.*, **15**, 296 (1996).
(19) W. Jia, R. Tchoudakov, E. Segal, R. Joseph, M. Narkis, and A. Siegmann, *Synth. Metal*, **132**, 269 (2003).
(20) J. Fournier, G. Boiteux, G. Seytre, and G. Marichy, *Synth. Metal,* **84**, 839 (1996).
(21) S. Vishal, A. N. Tiwari, and A. R. Kulkarni, *Mater. Sci. Eng.*, B **41**, 310 (1996).
(22) G. J. Li, X. Huang, J. K. Guo, and D. M. Chen, *Ceram. Inter.*, **28**, 623 (2002).
(23) G. Chen, W. Wang, D. Wu, and C. Wu, *Eur. Polym. J.*, **39**, 2329 (2003).
(24) M. Jacob, S. Thomas, and K. Varughese, *Composites Sci.Tech.*, **64**, 955 (2004).